Journal of Nuclear Materials 399 (2010) 167–174

Contents lists available at ScienceDirect

Journal of Nuclear Materials

journal homepage: www.elsevier.com/locate/jnucmat

Preparation of SiC_f/SiC composites by the slip infiltration and transient eutectoid (SITE) process

Saša Novak *, Goran Dražić, Katja König, Aljaž Iveković

Department for Nanostructured Materials, Jožef Stefan Institute, Slovenian Fusion Association (SFA) EURATOM-MHEST, Slovenia

ARTICLE INFO

Article history:
Received 25 August 2009
Accepted 17 January 2010

Keywords:
Fusion
SiC
Ceramic-matrix composite
Ceramic processing
Electrophoretic deposition

ABSTRACT

A novel ceramic processing route "SITE", composed of ceramic slip infiltration in a SiC-fibre preform and the low-temperature sintering of a SiC-based matrix using a transient eutectoid, has been introduced as an optional way of producing low-activation, SiC-based, ceramic-matrix composites for fusion applications. The matrix material's composition was developed on the basis of sintering studies using submicron and nanosized SiC powders and various low-activation precursors for the transient eutectoid secondary phase. Three different compositions of the secondary phase were investigated: SiO_2–Y_2O_3–P_2O_5, SiO_2–MgO–P_2O_5 and SiO_2–Al_2O_3–P_2O_5. The last of these resulted in the most promising material, which was obtained by sintering in controlled atmospheres at temperatures up to 1400 °C, where the SiC-fibres were prevented from losing their original properties. The matrix-material samples were characterised for their phase compositions. The SiC-fibre preform was infiltrated with the matrix material by using electrophoretic deposition. A stable and well-dispersed aqueous suspension enabled the efficient infiltration and preparation of a SiC_f/SiC composite with a relatively high density. The simple and rapid SITE processing technique appears to offer a viable, low-cost alternative to the methods presently used to produce low-activation SiC_f/SiC composites.

1. Introduction

SiC-based ceramic-matrix composites are the most attractive options for the structural and functional materials to be used in future fusion reactors, since they are non-magnetic and, in comparison with other proposed materials, they will constitute the least amount of radioactive waste. Furthermore, due to their good high-temperature resistance they can be used at temperatures as high as 1200 °C. Techno-economic studies have shown that the high efficiency levels required in a commercial reactor can only be achieved if the first-wall blanket is able to operate at temperatures approaching or exceeding 1000 °C. By comparison, the current design of the ITER calls for the use of specially developed reduced activation steels, notably the Eurofer steels, which offer good structural integrity, toughness and physical properties, at a somewhat reduced activation, but can only be used up to about 550 °C. This is considered to be adequate for the experimental conditions to which ITER will be subjected, but inadequate for future reactors, which are expected to produce energy on a commercial basis. Hence, the set of crucial properties that such a material is expected to offer is: a maximum use temperature of over 1000 °C, a low-activation in neutron irradiation, a high wear resistance under the conditions of service, a sufficient toughness to ensure operational structural reliability, a resistance to structural or lattice damage due to the impinging high-energy neutrons, a sufficient thermal conductivity, a gas impermeability, etc. [1–4].

Of the wide range of available materials, silicon carbide best meets these requirements. However, like every advanced, monolithic ceramic, SiC exhibits a low toughness (about 5 MPa $m^{-1/2}$ at best), and therefore a composite material of SiC-fibres in a SiC matrix appears to be a better alternative, as it offers a toughness of over 15 MPa $m^{-1/2}$ and a much higher reliability [5,6]. SiC-fibre-reinforced composites have shown superior reliability in many demanding applications under extreme conditions, like in gas-turbines engines, thermal barriers, armour, etc. However, in these applications, the materials are exposed to much less severe conditions than in a fusion reactor and, for example, open porosity and the presence of elements that activate strongly in a neutron flux do not represent a serious drawback, and therefore in their present form they cannot be considered as fusion-relevant materials. Namely, in addition to good mechanical properties, a sufficient gas tightness and a low neutron activation are among the key requirements for the structural applications, that are, however, rather difficult to achieve due to the intrinsic properties of the SiC. On the other hand, SiC_f/SiC composites have also been proposed for use as flow-channel inserts (concept "C") [2], where the hermeticity is not essential, while the thermal conductivity has to be minimized, as opposed to just being structural material.

* Corresponding author. Tel.: +386 1 477 3271; fax: +386 1 426 3126.
E-mail address: sasa.novak@ijs.si (S. Novak).

0022-3115/$ - see front matter © 2010 Elsevier B.V. All rights reserved.
doi:10.1016/j.jnucmat.2010.01.014

The processing of SiC_f/SiC is a complex, multi-stage process. The fibres are woven in a number of ways into a preform (ideally 3-dimensional), which is then infiltrated with a SiC-based matrix, leading to a certain degree of densification. Although many methods have been attempted in the past, no adequate solution has yet been presented. The current method of choice is chemical vapour infiltration (CVI). This method enables the production of pure SiC with a very low neutron activation, but it suffers from some processing drawbacks, notably the very long time required to build up sufficient material for the matrix, resulting in very high costs, and an inability to eliminate all the porosity, at the micro as well as the macro level. Although for most applications of SiC_f/SiC made with CVI such drawbacks are not crucial, they are critical in the case of the proposed fusion applications, where the porosity and gas-permeability must be reduced to zero and the thermal conductivity needs to be maximised [4].

Similarly, polymer infiltration and pyrolysis (PIP) that is based on the infiltration of a SiC-preform with a liquid preceramic polymer precursor, also fails to completely fill the gaps between the fibres and hence results in a material with an unacceptable residual open porosity. Attempts have been made to combine the technique with pressure-assisted slurry infiltration prior to the polymer infiltration [7]; however, the current state of the art suggests that suitable material properties cannot be achieved.

The third main group of processing techniques follows a ceramic route. Due to the covalent bonding being also responsible for the extraordinary properties of the SiC, the densification represents a demanding task. It is achieved either by solid-state sintering using boron as an additive, which is undesirable in fusion-relevant materials, or liquid-phase sintering (LPS) using metal oxides as the sintering additives, typically Al_2O_3–Y_2O_3 [8–11]. The temperatures needed for both the solid-state and liquid-phase sintering, even if combined with high pressures, easily exceed the temperature range that the present grades of SiC-fibres can withstand without serious damage, [12,13]. Pressure-less, high-temperature densification, typically performed above 1900 °C, is also associated with a β- to α-SiC transformation and certain shrinkage that limits the possibility to prepare a gas-impermeable composite material. The most developed technique appears to be the "NITE" process (nano-powder infiltration and transient eutectoid) [14], which may, according to the literature data, produce a material with a high density and a relatively high mechanical strength. In the NITE process, alumina and yttria are used as the sintering aids, and the final densification is achieved by hot pressing.

In the present work we report on the development of an alternative technique for the fabrication of a dense, low-activation, fusion-relevant, SiC-based material densified at moderate temperatures. The so-called "SITE" process is based on slip infiltration and the use of a transient eutectoid that makes it, in a way, related to the NITE process, although in the SITE the electrophoretic deposition (EPD) of the stable colloid suspension for infiltration of the SiC-preform with SiC powder is employed and the densification takes place at significantly lower temperatures. At the sintering temperatures used in this study the extent of the transformation of SiC-3C to SiC-6H was expected to be negligible. The sintered materials were comprehensively characterised by SEM, TEM, EDXS and XRD for their structural properties.

2. Experimental

The starting materials for the matrix were β-SiC powder BF12 (H. Starck, Germany) with a mean particle size of 0.5 μm and a nanosized β-SiC powder Hefei (30 nm, Hefei Kiln Nanom. Technol. Dev., China). The compositions of the sintering additives were selected according to the relative activation of the elements given in the database FISPACT 2005, EASY, ENDF/B-VI.8, EAF 2005 [15] and the available phase diagrams. In this work we used an aluminium dihydrogen phosphate solution (TKK Hrastnik, Slovenia) and MgO and Y_2O_3 powders (Alfa Aesar, J. Matthey, USA). In some experiments the SiC powder was coated with a thin Al-, Mg- or Y- hydroxide layer, using a procedure described elsewhere [16]. In the present work we report on seven differently prepared SiC-based ceramics with the compositions summarised in Table 1.

Table 1
The starting compositions of the matrix materials with different sintering aids.

Sample	SiC powder	Secondary phase	Precursor
Y1	BF12	SiO_2–Y_2O_3–P_2O_5	Oxide powders
Y2	BF12	SiO_2–Y_2O_3–P_2O_5	(Y_2O_3 + P_2O_5)-coating
M1	BF12	SiO_2–MgO– P_2O_5	Oxide powders
M2	BF12	SiO_2–MgO– P_2O_5	(MgO + $MgHPO_4$)-coating
A1	BF12	SiO_2–Al_2O_3– P_2O_5	$Al(H_2PO4)_3$ solution
A2	BF12	SiO_2–Al_2O_3– P_2O_5	(AlOOH + P_2O_5)-coating
A3	Hefei (nano)	SiO_2–Al_2O_3– P_2O_5	$Al(H_2PO4)_3$ solution

Aqueous suspensions of the powders were homogenised by mixing in polymer containers with Teflon-coated balls or dispersed with an ultrasonic finger processor with an acoustic power density of 10^9 W/m^2 for 5 min (Hielscher Ultrasonics, Germany). Special care was taken to minimize the contamination with metallic impurities, which may strongly activate in a neutron flux. For the matrix sintering studies, from suspensions with a total loading of up to 60 wt.%, plate-shaped green parts were formed by electrophoretic deposition [17]. The samples were sintered in a protective atmosphere (Ar, 99.999%) at a temperature in the range from 1300 to 1400 °C.

For the infiltration experiments, 3-D Nicalon SA fabrics without an interface layer were used. The infiltration with the SiC powder suspension was carried out with the help of an electric field. The electrophoretic deposition (EPD) experiments were performed with freshly prepared aqueous suspensions at a constant voltage of 60 V; the distance between the square-shaped electrodes (20 mm × 20 mm) was 20 mm. More details are described in our previous papers [17,18]. After the deposition, the infiltrated preform was carefully removed from the cell, dried in air and subsequently vacuum infiltrated with an $Al(H_2PO_4)_3$ solution. The dried composite parts were sintered at 1400 °C for 1 h in an argon atmosphere.

After sintering, the materials were examined by optical and scanning electron microscopy (Jeol JSM-840A and Jeol JSM-5800). High-resolution transmission electron microscopy (Jeol 2010F FEG TEM/STEM), EDXS (Isis 300 from Oxford Instruments), electron energy-loss spectroscopy (Gatan PEELS 677), high-angle annular dark-field detector imaging and electron nanodiffraction were used to characterise the chemical composition of the phases present and their crystal structure. The crystal structure and the amount of amorphous phase in the sintered samples were characterised by XRD (Bruker AXS D4 Endeavor diffractometer using Cu Kα radiation) using the Rietveld method [19].

3. Results and discussion

3.1. Selection of the sintering additive

Low-activation elements that form a eutectic phase in the temperature interval that does not jeopardize the integrity of the SiC-fibres were selected in accordance with the FISPACT database [15]. The relative activity for SiC and the selected candidate elements for 1 kg of matter as a function of time after irradiation, based on FISPACT 2005, EASY – European Activation System, are illustrated in Fig. 1. [20] The calculation is for a neutron flux of 10^{17} n/s m^2

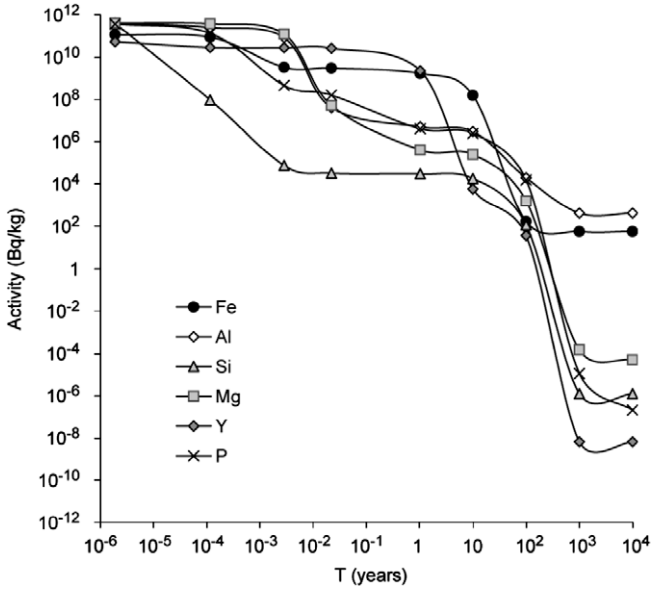

Fig. 1. Relative activity of elements, potentially applicable as a matrix sintering aid, as a function of time after irradiation (FISPACT 2005, EASY, ENDF/B-VI.8, EAF 2005; calculation is for neutron flux 10^{17} n/s m^2 and for time of irradiation 1 week).

and for an irradiation time of 1 week. It is clear that the iron, which was added for comparison as the major constituting element of Eurofer, exhibits a rather high short-term as well as longer-term activation. Aluminium has a lower short-term activation, but due to the formation of Al^{26} it remains active for thousands of years, while yttrium activation is proposed to decrease significantly after just several years. Accordingly, the SiC-ceramics prepared by liquid-phase sintering using a conventional transient liquid phase SiO_2–Al_2O_3–Y_2O_3 are expected to activate only slightly less than the Eurofer. The diagram also implies that Mg and P have a low-activation and hence represent possible alternatives to the conventional sintering additive. According to the phase diagrams, the MgO and Al_2O_3 form a eutectic with P_2O_5 and SiO_2 in the range of moderate temperatures, i.e., below 1500 °C, which gives us the potential to attain a SiC-based matrix with low porosity at temperatures where the SiC-fibres retain their properties and the SiC grains remain predominantly in the form of the β-phase.

3.2. Ceramic-matrix

In order to verify the properties of the matrix material composed of the SiC powder and sintering additives, for which the compositions were selected on the basis of the above assumptions, we first prepared samples of the ceramic-matrix without fibres. It is well known that SiO_2 naturally covers the surface of SiC powder and is also one of the secondary-phase constituents. As illustrated in the high-resolution transmission electron micrographs (HRTEM) in Fig. 2a and b, the SiO_2 is present as an approximately 2-nm-thick amorphous layer at the surface of the as-received SiC particles. The submicron SiC powder (BF12) contained 0.78 wt.% oxygen, while due to the larger surface area, the nanosized powder (Hefei) contained as much as 1.8 wt.% oxygen. Furthermore, the comprehensive analyses of the oxygen content as a function of processing parameters revealed that heating the submicron powder in argon with 99.999% purity results in an increase in oxygen content up to 2.87% (for the submicron powder) and to 1.3% in high-purity argon (99.9999%) [16,21]. Hence, we proposed that a sufficient amount of SiO_2 for the secondary phase is naturally available on the surface of the SiC powders and that it can be controlled by the processing parameters.

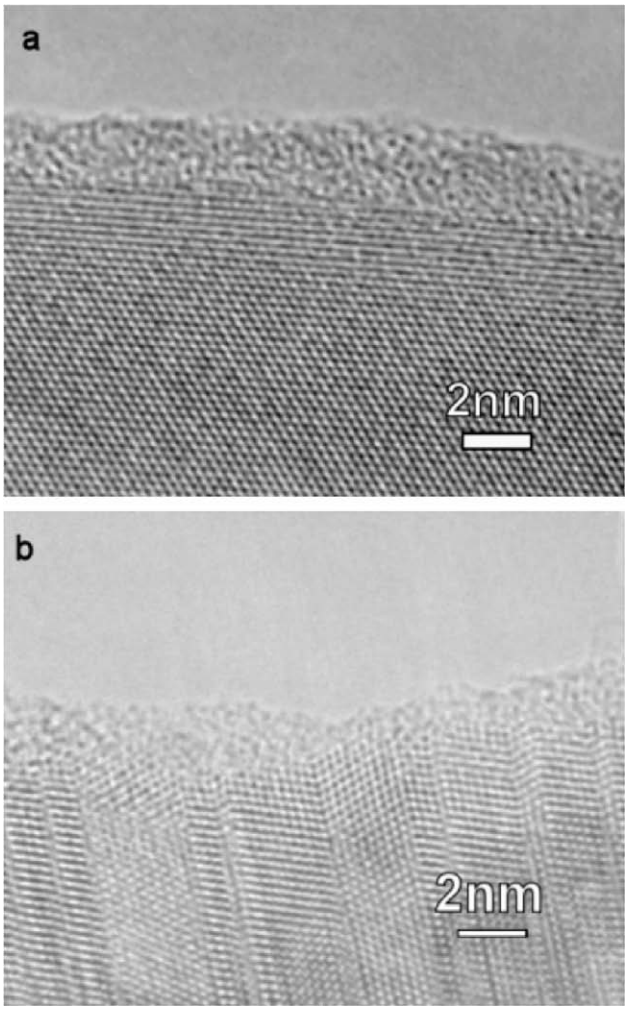

Fig. 2. HRTEM micrographs of the: (a) submicron and (b) nanosized SiC particles with a thin layer of SiO_2 on the surface.

In addition to the naturally present SiO_2 for the secondary phase in the SiC-based matrix, MgO, Y_2O_3 or Al_2O_3 were added as well as a small amount of P_2O_5, whose role is to temporarily decrease the melting temperature of the eutectic phase. After a certain amount of time during the sintering process the phosphorus evaporates from the system. The starting compositions of the secondary phases are summarised in Table 1. It is also evident from Table 1 that the metal oxides were added in different forms: either as a powder mixture or as an aqueous solution, or they were applied as a thin layer on the SiC particle surfaces in a special coating process [16,22].

3.2.1. SiO_2–Y_2O_3–P_2O_5

In contrast to the conventional secondary phase for the liquid-phase sintering of SiC that contains silica, yttria and alumina, in our matrix-material samples the alumina was substituted with phosphorus oxide. Two different processing routes were employed: (a) the homogenisation of the powder mixture (SiC and oxide powders) and (b) the coating of the SiC powder with the sintering-aid precursor (see Table 1). The corresponding SEM micrographs of the sintered samples Y1 and Y2 are presented in Fig. 3a and 3, respectively. The coated powder obviously resulted in a better yttria distribution (white particles in Fig. 3b) than in the samples prepared from the powder mixture (Fig. 3a); however, both samples sintered at 1400 °C reveal a certain amount of residual

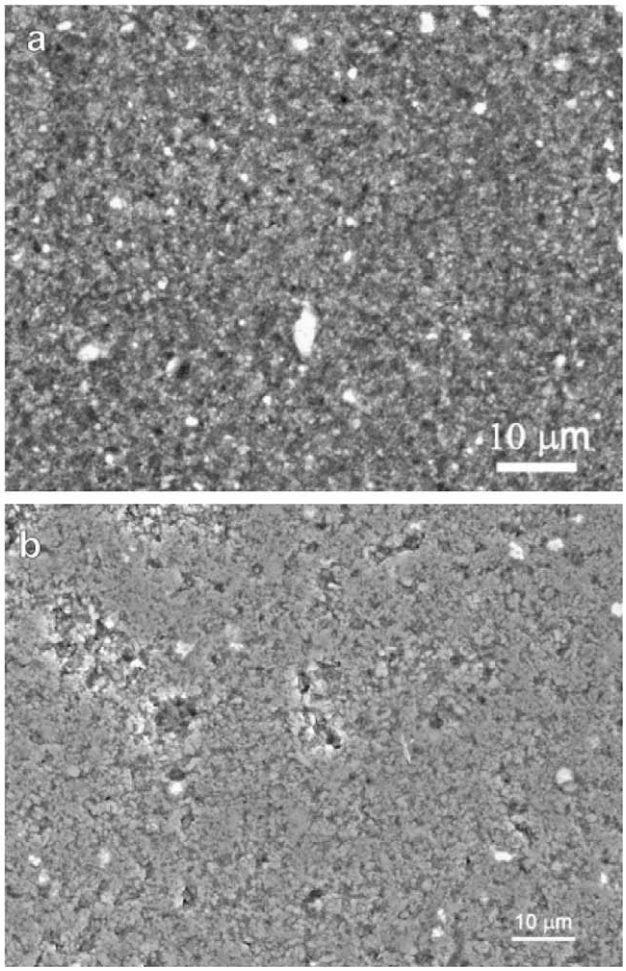

Fig. 3. Scanning electron micrographs of the sintered matrix samples Y1 (a) and Y2 (b) prepared from the powders or from the yttria-coated SiC, respectively.

porosity. It is reasonable to speculate that a higher density could be achieved by hot pressing.

3.2.2. SiO_2–MgO–P_2O_5

The characteristic microstructures of the samples with the MgO-containing secondary phase (M1 and M2, cf. Table 1) after sintering in argon are illustrated in Fig. 4a–c. The sample M1, prepared from the MgO-containing powder mixture, was highly porous (Fig. 4a), which may be ascribed to the chemical reaction of SiC with MgO. Namely, according to literature data [23], in a reducing atmosphere the SiC reacts with MgO to form gaseous products by two possible reactions:

$$SiC + 2MgO \Rightarrow SiO_{(g)} + 2Mg_{(g)} + CO_{(g)}$$
$$SiC + MgO \Rightarrow MgSiO_{3(l)} + 3Mg_{(g)} + CO_{(g)}$$

In our case, the atmosphere was not reducing, but obviously the reaction took place to some extent also during the sintering in argon. For comparison, we also sintered the samples in air and the resulting porosity was strongly reduced (see Fig. 4b). As expected, in this case the amount of amorphous phase increased (the results are presented in a subsequent section, Table 3). This implies that the MgO might be a suitable sintering additive for the densification of SiC, providing that a properly balanced atmosphere is used in order to minimize the amount of amorphous phase and at the same time to minimize or avoid the reaction of MgO with SiC.

The sample M2 was prepared from the SiC powder coated with a layer of $MgHPO_4$ and sintered in argon. The comparison of the

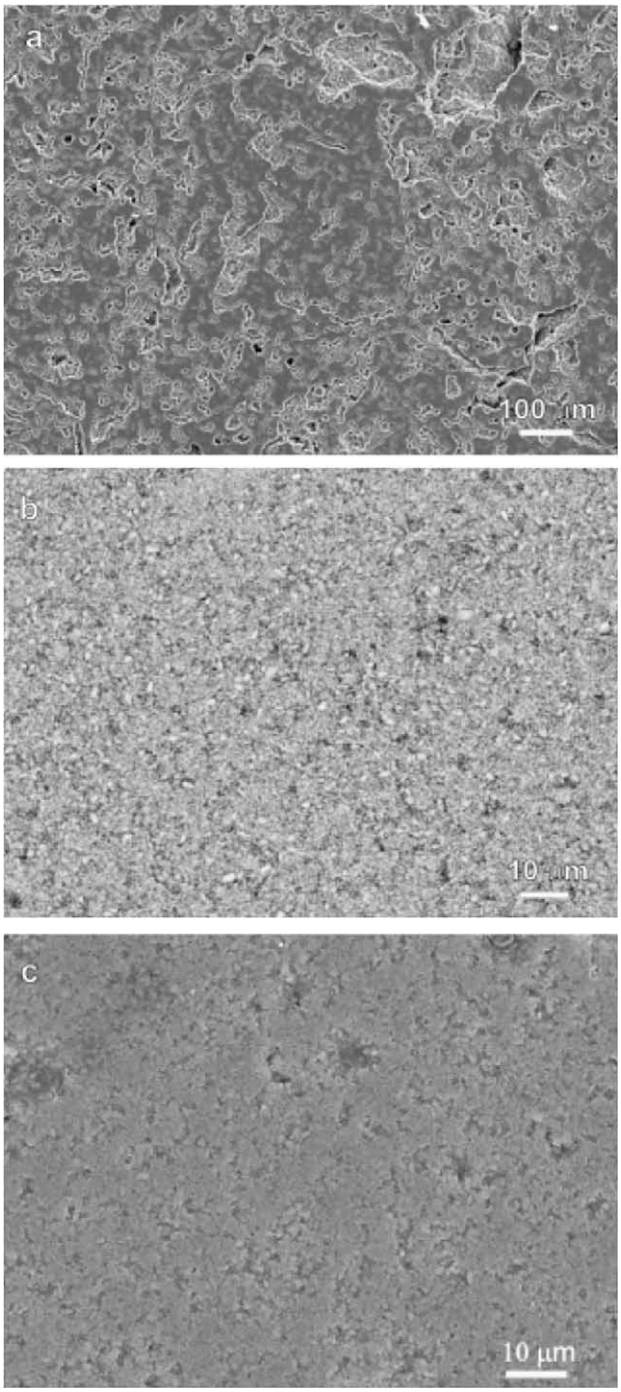

Fig. 4. Scanning electron micrographs of the matrix samples M1 (a), M2 (b) and M3 (c) sintered in Ar (M1 and M3) or in air (M2).

resulting microstructure, illustrated in Fig. 4c, with that in Fig. 4a, confirms the beneficial effect of the coating. The MgO-coated SiC powder resulted in a lower porosity than that observed for the sample prepared from the powder mixtures, which is due to the more homogeneous distribution of the sintering additive. A certain degree of porosity is still present, most probably as a consequence of the above-mentioned reaction.

3.2.3. SiO_2–Al_2O_3–P_2O_5

In the third set of samples the conventional composition of the eutectic phase was modified by replacing the Y_2O_3 with P_2O_5. In

this case, the precursor for the transient liquid phase was either added as a solution of $Al(H_2PO_4)_3$ (A1 and A3, cf. Table 1) or in the form of a thin layer of boehmite AlO(OH) applied to the SiC particles (sample A2) [16]. Both techniques resulted in apparently dense microstructures, with the particle size estimated to be approximately 1 μm, as illustrated in Fig. 5a. Since the densification took place mostly by viscous-flow sintering, where the particles are rearranged in the transient liquid phase, no major grain growth was observed. In addition to the samples A1 and A2 that were prepared from submicron SiC powder, the sample A3 was prepared from the nanosized Hefei powder. The resulting highly dense microstructure with a grain size below 1 μm is presented in Fig. 5b.

An EDS analysis of the sample A1 revealed that the composition of the phosphate-containing binder phase changed during the firing in an inert atmosphere. After forming the transient liquid phase, the phosphate reduces to form phosphorus, which evaporates and condenses in the cold trap in the furnace. Consequently, the sintered material contains less than 0.5 wt.% phosphorus phase. Furthermore, the EDS analysis also revealed the presence of a small amount of aluminium, <2 wt.% (Fig. 5c). As presented in the transmission electron micrograph of the sample A1, Fig. 6, the SiC particles are embedded in an amorphous secondary phase (G). Small mullite (M) particles were also found.

3.2.4. Phase composition of the sintered matrix material

The phase composition of the sintered matrix materials was analysed by XRD using the Rietveld refinement method using an internal standard [19,24]. Special attention was paid to the possible phase transformation of SiC, from cubic 3C (β-SiC) to the hexagonal 6H (α-SiC), and to the amount of amorphous secondary phase in the sintered samples. It has to be pointed out here that the secondary phase was formed from the amorphous silica on the surface of the starting SiC powder (see Fig. 2) and from the sintering additives. In order to estimate both contributions, the phase compositions of the starting SiC powders were also analysed for comparison. The phase compositions of the powders are presented in Table 2, while the results for the sintered samples are listed in Table 3.

The submicron-sized SiC powder was determined to contain mostly the cubic (3C) and 8.6% of the hexagonal (6H) phase (see Table 2). The XRD analysis of the powders also revealed the presence of 11% of amorphous phase, which could be partly explained by the above-shown silica layer on the particles. In contrast to the submicron SiC powder, the nanosized powder contained only the cubic phase, but the amount of amorphous silica phase was much higher, i.e., 25.3%. As presented in both cases, the amorphous phase can only be partly eliminated by dissolution in HF.

Table 3 summarises the phase compositions of the sintered matrix materials prepared using different secondary-phase compositions. As expected, the 3C phase remains as the prevailing phase, which confirms that due to the moderate temperature regime used, no phase transformation of the cubic SiC (3C) to the hexagonal (6H) appeared. The results also show that the sintered samples A1 and A3, which were prepared by the same procedure, but from the submicron or nanosized SiC powder, respectively, contained only a slightly larger amount of the amorphous silica-based secondary phase than the starting powder. This implies that the majority of the amorphous phase in the sintered material results from the silica layer on the starting SiC powder, while the contribution of the sintering aids is relatively small.

The amount of amorphous phase also appeared to depend largely on the processing conditions: although the coating of the SiC powder with sintering additive precursors showed a beneficial effect on the density of the matrix materials, the amount of amorphous phase content did not decrease, even an increase was observed. This can be explained by the larger amount of oxygen introduced during the coating procedure. As expected, sintering in the open air instead of the protective atmosphere resulted in a significantly higher content of amorphous phase.

Hence, the results of EDS and XRD analysis of the SiC-matrix-material samples indicate that the composition of the eutectic phase for liquid-phase sintering could be adapted to achieve sinterability at lower temperatures than required for the conventional compositions, which would preserve the fibres from deterioration

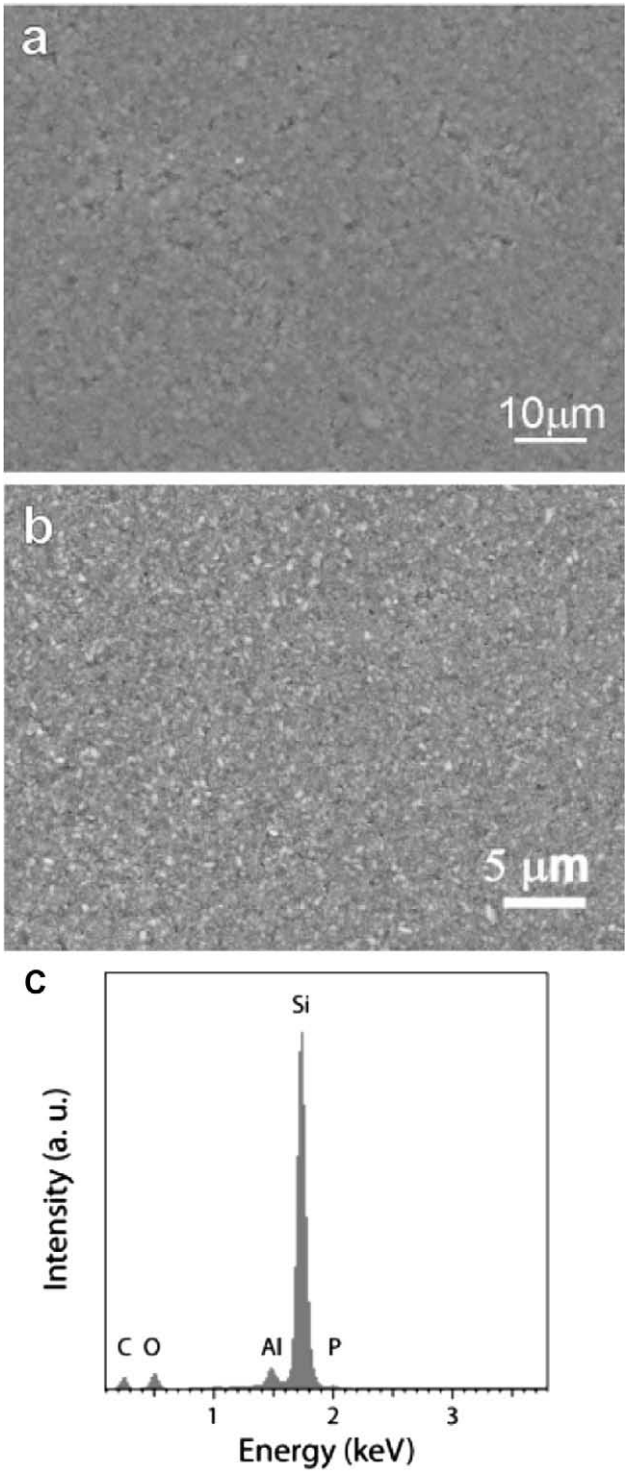

Fig. 5. SEM micrograph of the sintered matrix samples A1 (a) and A3 (b) and EDS spectrum of the sample A1 (c).

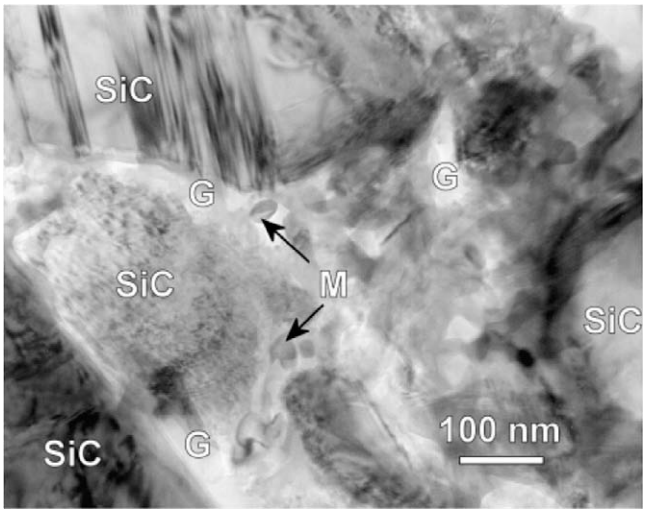

Fig. 6. TEM micrograph of the sintered matrix samples A1.

Table 2
Phase compositions of the SiC starting powders used in this investigations.

SiC powder	Cubic SiC (3C) (%)	Hexagonal SiC (6H) (%)	Amorphous phase (%)
BF12	80.4	8.6	11
Washed with HF	83.3	9.6	7.1
Hefei (nano)	74.7	–	25.3
Washed with HF	80.9	–	19.1

and the SiC powder from the β-SiC (cubic) to α-SiC (hexagonal) transformation. The lowest porosity, and at the same time the smallest amount of amorphous phase, was obtained for the matrix composition A1, which was, accordingly, used in a further study to prepare the SiC-fibre-reinforced composite. Due to twice as much amorphous phase content in the sample with nanoSiC (A3), the use of this powder was omitted.

3.3. Infiltration of SiC-fibre fabric

In the next step, the matrix material was introduced into the SiC-fibre performs. This was done in an electric-field-assisted colloidal process, where the charged particles in the aqueous suspension are forced to move toward the oppositely charged electrode through the SiC-fibre fabric preform (see Fig. 7). The surface charge on the SiC-fibres, determined by the analysis of the electrokinetic mobility of the crushed SiC-fibres, revealed a negative net-charge over a wide range of pH values [18], which favours the anodic deposition. Hence, the negatively charged SiC-preform was dipped in the alkaline suspension of the highly negatively charged SiC powder (zeta-potential: −60 mV). After applying the voltage, the SiC particles migrated towards the anode placed behind the preform. The fabric holder was tightly sealed in order to force the particles to migrate through the fabric and fill it gradually. Following a mechanism proposed elsewhere [18], it is considered that the particles first deposit on the membrane, forming a thin (up to 0.5 mm) deposit and then gradually fill the fabric in front of the membrane. After impregnating the preform, the SiC particles finally formed a deposit on the front side of the fabric.

The powder-infiltrated samples were further vacuum infiltrated with the $Al(H_2PO_4)_3$ solution, carefully dried and sintered at 1400 °C in an argon atmosphere. The sintered samples were cut and the polished cross-sections observed with an optical microscope in polarised light and with an SEM. The microstructures of the cross-sections are presented in Fig. 8a and b. As illustrated in Fig. 8b, on their way to reach the electrode behind the fibre preform, the electrostatically separated and well deagglomerated SiC

Table 3
Phase compositions of the sintered matrix-material samples with various compositions.

Sample	SiC (3C) (wt.%)	SiC (6H) (wt.%)	SiO_2 (crystoballite) (wt.%)	SiO_2 (quartz) (wt.%)	$Al_6Si_2O_{13}$ (mullite) (wt.%)	Amorphous phase (wt.%)
Y2	64.4	8.4	1.2	1		24.9
M1	77	9	2.7	0.7		10.7
M2	68.3	8.4	1.7	0.3		21.3
M2 (air)	56.4	7.2	1.5	0.9		34
A1	70.25	7.4	4.39	0.73	5	12.2
A2	63.36	7.93	6.26	1.24	5.39	15.8
A3	64.19	–	6.41	1.26		28.1

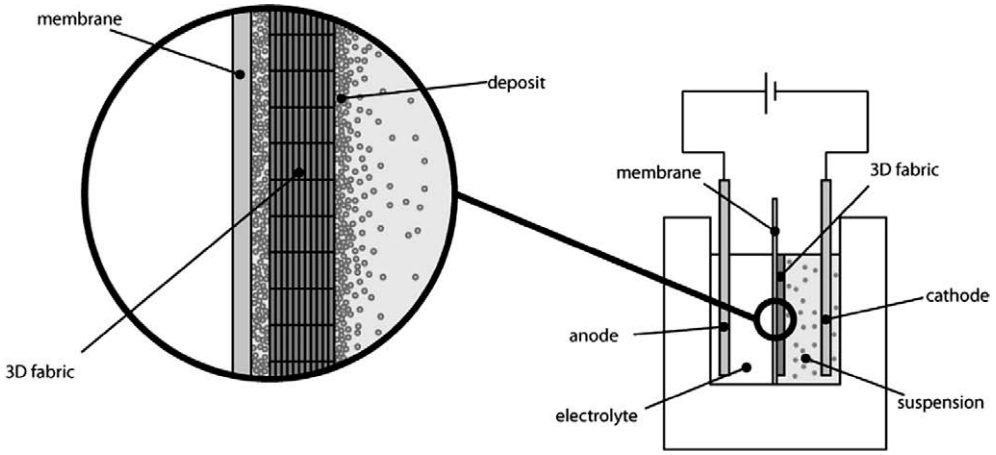

Fig. 7. Schematic of the electrophoretic infiltration of the SiC-fibre preform with SiC-matrix material suspension.

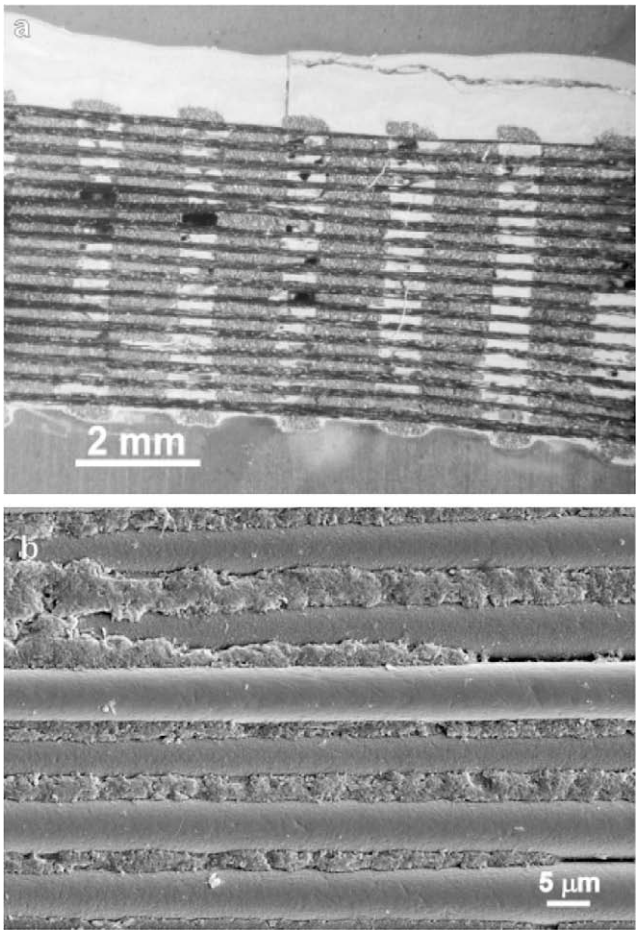

Fig. 8. Optical (a) and SEM micrographs (b) of the cross-section of the infiltrated SiC-fibre preform (the bottom side was attached to the deposition electrode) before and after sintering.

particles were able to migrate even through relatively narrow gaps between the individual fibres in the tows and hence gradually fill the voids throughout the whole thickness of the 4 mm-thick SiC-fibre preform. Some larger voids remained unfilled, however, which is ascribed to trapped air bubbles in the preform during the infiltration. These can presumably be eliminated by careful pre-treatment of the preform, which will be explored in our future work.

4. Conclusions

Based on the FISPACT 2005 EASY database and phase diagrams, magnesia, yttria and alumina were selected as sintering additives for the low-temperature sintering of a SiC-matrix material. A small amount of P_2O_5 was employed as a transient additive that lowers the viscosity of the secondary phase during the particles' rearrangement process, while silica, found in a thin layer on the particles' surfaces, acts as the third component for the secondary phase in the system $MeO–SiO_2–P_2O_5$ (Me stands for Y, Mg or Al). Various procedures were used for the preparation of the matrix ceramics. As expected, the samples prepared from the coated powders were more homogeneous and exhibited a lower porosity than those prepared by mixing the powders. The amount of the secondary phase did, however, increase slightly.

The microstructural observations of the matrix-material samples sintered using different additives confirmed that the P_2O_5 significantly decreases the densification temperature and, after playing its role in viscous-flow sintering, it evaporates. The samples with the MgO addition sintered in an argon atmosphere were highly porous due to the reaction of the MgO with SiC forming gaseous products, while sintering in the open air resulted in dense ceramics with a large amount of silica-rich amorphous secondary phase. The system $Y_2O_3–P_2O_5–SiO_2$ did not result in dense ceramics; it is, however, supposed that hot pressing might result in sufficient densification. Due to a moderate temperature sintering regime, i.e., below 1500 °C, no transformation from cubic to hexagonal SiC appeared.

The lowest porosity for the matrix material was obtained with a secondary phase of $Al_2O_3–P_2O_5–SiO_2$, which was therefore used in the fabrication of the fibre-reinforced composite. The SiC-fibre preform was first infiltrated with a silicon carbide powder suspension employing the electrophoretic deposition technique that was followed by the vacuum infiltration of an aqueous solution of Al-phosphate and sintering at 1300–1400 °C. The results suggested that the presented technique offers a promising way for producing SiC-fibre-reinforced SiC ceramics in a moderate temperature regime.

The presented SITE process (slip infiltration and transient eutectoid) that is composed of a two-stage infiltration followed by a moderate temperature densification offers the possibility to adapt the composition to better fit the expected neutron activation and might hence serve as a promising gateway to a suitable fusion-relevant material. Further investigations will be directed at minimising the oxide-rich secondary phase as well as in tailoring the material's properties for application as flow-channel inserts.

Acknowledgements

This work, supported by the European Communities under the Contract of Association between EURATOM and the Ministry of Higher Education, Science and Technology of the Republic of Slovenia, was carried out within the framework of the European Fusion Development Agreement. The content of the publication is the sole responsibility of its authors and it does not necessarily represent the views of the Commission or its services.

The work was also supported by the Slovenian Research Agency (project No. J2-7506-01016) and by the National Research Programme P2-0084. Parts of the work were performed in the diploma studies of Mrs. N. Drnovšek (sintering studies) and Mrs. S. Ovtar (XRD analysis) and the PhD studies of Mrs. Katja König and Mr. Aljaž Iveković.

References

[1] R. Lässer, N. Baluc, J.-L. Boutard, E. Diegele, S. Dudarev, M. Gasparotto, A. Möslang, R. Pippan, B. Riccardi, B. van der Schaaf, Fusion Eng. Des. 82 (2007) 511.
[2] R. Andreani, E. Diegele, W. Gulden, R. Lässer, D. Maisonnier, D. Murdoch, M. Pick, Y. Poitevin, Fusion Eng. Des. 81 (2006) 25.
[3] R. Naslain, Comp. Sci. Technol. 64 (2004) 155.
[4] A. Hasegawa, A. Kohyama, R.H. Jones, L.L. Snead, B. Riccardi, P. Fenici, J. Nucl. Mater. 283–287 (2000) 128.
[5] R.H. Jones, L. Giancarli, A. Hasegawa, Y. Katoh, A. Kohyama, B. Riccardi, L.L. Snead, W.J. Weber, J. Nucl. Mater. 307–311 (2002) 1057.
[6] R.H. Jones, C.H. Henager Jr., J. Eur. Ceram. Soc. 25 (2005) 1717.
[7] C.A. Nannetti, A. Ortona, D.A. de Pinto, B. Riccardi, J. Amer. Ceram. Soc. 87 (2004) 1205.
[8] S. Prochazka, The Role of Boron and Carbon in the Sintering of Silicon Carbide, in: P. Popper (Ed.), Special Ceramics, vol. 6, The British Ceramic Research Association, 1975, p. 171.
[9] K. Negita, J. Am. Ceram. Soc. 69 (12) (1986) 308.
[10] K. Biswas, G. Rixecker, I. Wiedmann, M. Schweizer, G.S. Upadhyaya, F. Aldinger, Mater. Chem. Phys. 67 (2001) 180.
[11] G. Magnani, L. Beaulardi, L. Pilotti, J. Eur. Ceram. Soc. 25 (2005) 1619.
[12] T. Toplišek, G. Dražić, S. Novak, S. Kobe, Scanning 30 (2008) 35.
[13] M. Takeda, Y. Imai, H. Ichikawa, N. Kasai, T. Seguchi, K. Okamura, Compos. Sci. Technol. 59 (1999) 793.
[14] Y. Katoh, A. Kohyama, T. Nozawa, M. Sato, J. Nucl. Mater. 329–333 (2004) 587.

[15] R.A. Forrest, UKAEA FUS 513, EURATOM/UKAEA Fusion, The European Activation System: EASY-2005 Overview, January 2005. <http://www.fusion.org.uk/techdocs/ukaea-fus-513.pdf>.
[16] S. Novak, J. Kovač, G. Dražić, J.M.F. Ferreira, S. Quaresma, J. Eur. Ceram. Soc. 27 (2007) 3545.
[17] S. Novak, K. Rade, K. König, A.R. Boccaccini, J. Eur. Ceram. Soc. 28 (2008) 2801.
[18] S. Novak, K. König, A. Iveković, A.R. Boccaccini, Key Eng. Mater. 412 (2009) 237.
[19] H.M. Rietveld, J. Appl. Cryst. 2 (1969) 65.
[20] I. Lengar, L. Snoj, P. Rogan, M. Ravnik, S. Novak, G. Dražić, Evaluation of activation characteristics of silicon carbide in a fusion spectrum, in: S. Rožman, et al., (Eds), International Conference Nuclear Energy for New Europe 2008, Slovenia, September 8–11, 2008, p. 9.
[21] N. Drnovšek, Development of SiC-Based Material for Fusion Application, Diploma Work (in Slovene), University of Ljubljana, 2006.
[22] Z. Tatli, D.P. Thompson, J. Eur. Ceram. Soc. 27 (2007) 1313.
[23] D. Foster, D.P. Thompson, J. Eur. Ceram. Soc. 19 (1999) 2823.
[24] S. Ovtar, Quantitative Analysis of Amorphous Phase in SiC-Based Ceramics by Means of XRD Diffraction (in Slovene), Diploma Work, University of Ljubljana, 2007.